doi: 10.21495/71-0-319

25th International Conference
ENGINEERING MECHANICS 2019
Svratka, Czech Republic, 13 – 16 May 2019

ACOUSTIC WAVES IN FLUID-SATURATED PERIODIC SCAFFOLDS

E. Rohan [*], **R. Cimrman** [**]

Abstract: *We consider acoustic wave propagation in periodic scaffolds saturated by inviscid fluid at rest. To analyze the wave dispersion, two approaches are examined: the periodic homogenization (PH) and the Floquet-Bloch wave decomposition (FB). While PH gives dispersion-less response, the FB method enables to capture band gap behaviour.*

Keywords: Acoustics, Periodic scaffolds, Floquet-Bloch theory, Homogenization, Band gaps.

1. Introduction

Modelling of acoustic waves in fluid saturated porous media has been treated mostly using the homogenization theory (Sanchez-Palencia, 1980), or using the phenomenological models using the theory of porous media. In this paper, we report on the acoustic wave dispersion in periodic scaffolds constituted by sintered ceramic fibres. Waves in theses elastic structures were studied recently by Kruisová et al. (2018) without effects of the fluid. Here we consider waves propagating in a fluid saturating these periodic structures (scaffolds) while neglecting their compliance. The dispersion analysis is based on a model obtained using the Floquet-Bloch theory, cf. Collet et al. (2011), enabling to analyze wave of lengths comparable with the periodicity size. For comparison, the lowest frequency modes are compared with the homogenization-based prediction.

We recall the Navier-Stokes equations for a homogeneous, slightly compressible viscous fluid, while thermal effects are disregarded (barotropic fluid). The fluid velocity $\boldsymbol{w}$ and pressure q satisfy

$$\rho_0 \left(\frac{\partial}{\partial t} \boldsymbol{w} + \boldsymbol{w} \cdot \nabla \boldsymbol{w} \right) = -\nabla q + \nabla \cdot \mathbb{D}\boldsymbol{e}(\boldsymbol{w}) \ , \quad \gamma \left(\frac{\partial}{\partial t} q + \boldsymbol{w} \cdot \nabla q \right) = -\nabla \cdot \boldsymbol{w} \ , \tag{1}$$

where ρ_0 is the reference fluid density, γ is the compressibility, and $\mathbb{D}\boldsymbol{e}(\boldsymbol{w})$ represents the viscous stress given by the velocity strain $\boldsymbol{e}(\boldsymbol{w}) = 1/2(\nabla \boldsymbol{w} + (\nabla \boldsymbol{w})^T)$ and by the viscosity tensor, $\mathbb{D} = (D_{ijkl})$ with $D_{ijkl} = \eta \delta_{ij}\delta_{kl} + \mu(\delta_{ik}\delta_{jl} + \delta_{il}\delta_{jk})$ depending on the 1st and the 2nd viscosities, μ and η, respectively. Since we are interested in acoustic waves, the total velocity and pressure fields can be decomposed into steady (denoted by bar) and fluctuating parts (denoted by tilde˜),

$$\boldsymbol{w} = \bar{\boldsymbol{w}} + \tilde{\boldsymbol{u}} \ , \quad q = \bar{q} + \tilde{p} \ . \tag{2}$$

In this paper, we confine to the acoustics of inviscid stationary fluids, the only velocity corresponds to the perturbations by the transmitted acoustic waves, *i.e.* $\bar{\boldsymbol{w}} = 0$ and $\mu = \eta = 0$.

2. Floquet-Bloch decomposition of waves in scaffolds saturated by inviscid fluid

We consider an infinite porous medium $\Omega \subset \mathbb{R}^3$ whose the periodic structure is generated by a representative periodic cell $\mathcal{Z} = \Pi_{i=1}^3]0, a_i[$ which is a block with edges a_i. The fluid occupies channels $\Omega_f \subset \Omega$ which are represented by $\mathcal{Z}_f \subset \mathcal{Z}$. Thus, the periodic cell $\mathcal{Z}$ consists of the fluid and solid parts separated by the

[*] Prof. Dr. Ing. Eduard Rohan, DSc.: NTIS New Technologies for Information Society, Department of mechanics, Faculty of Applied Sciences, University of West Bohemia, Univerzitní 8, 30614, Pilsen, CZ, e-mail: rohan@kme.zcu.cz
[**] Robert Cimrman, New Technologies - Research Centre, University of West Bohemia, cimrman3@ntc.zcu.cz

fluid-solid interface $\partial_s\mathcal{Z}_f$, such that $\mathcal{Z} = \mathcal{Z}_f \cup \mathcal{Z}_s \cup \partial_s\mathcal{Z}_f$. By $\partial_\#\mathcal{Z}_f = \partial\mathcal{Z}_f \setminus \partial_s\mathcal{Z}_f$ we denote the "periodic part" of the boundary, $\partial_\#\mathcal{Z}_f \subset \partial_\#\mathcal{Z}$. A $\mathcal{Z}$ periodic function attains the same values at the homologous points on opposite faces of $\partial_\#\mathcal{Z}$.

We consider the decomposition (2) and assume stationary inviscid fluid, *i.e.* $\bar{\boldsymbol{w}} = 0$. Assuming that γ and ρ_0 are constants, the fluid velocity field can be eliminated from the system (1), so that

$$\gamma\rho_0 \frac{\partial^2}{\partial t^2}\tilde{p} = \nabla^2\tilde{p}\ , \quad \text{in } \Omega_f\ , \quad \boldsymbol{\nu}^f \cdot \nabla\tilde{p} = 0\ , \quad \text{on } \partial_s\Omega_f\ , \tag{3}$$

where $\boldsymbol{\nu}^f$ designates the unit normal vector outward to $\mathcal{Z}_f$. By virtue of the Floquet-Bloch theory, the wave $\tilde{p}(t,x)$ propagating in an infinite medium is expressed in terms of a $\mathcal{Z}$-periodic function $p(x)$, such that

$$\tilde{p}(x,t) = p(x)e^{-\mathrm{i}\boldsymbol{\kappa}\cdot\boldsymbol{x}}e^{\mathrm{i}\omega t}\ , \quad \tilde{\boldsymbol{u}}(x,t) = \boldsymbol{u}(x)e^{-\mathrm{i}\boldsymbol{\kappa}\cdot\boldsymbol{x}}e^{\mathrm{i}\omega t}\ , \tag{4}$$

for $x \in \Omega_f$, where the wave vector $\boldsymbol{\kappa} = \varkappa\boldsymbol{n}$ is given by the wave direction $\boldsymbol{n}$ and the wave number $\varkappa$. Functions $\boldsymbol{u}$ and p are $\mathcal{Z}$-periodic and $\boldsymbol{u}\cdot\boldsymbol{\nu}^f = 0$ on $\partial_s\mathcal{Z}_f$. Let $H^1_\#(Y)$ denotes the Sobolev space of weakly differentiable Y-periodic functions defined in Y. The following space of $\mathcal{Z}$-periodic functions p is used (note $\nabla(qe^{-\mathrm{i}\boldsymbol{\kappa}\cdot\boldsymbol{x}}) = (\nabla q - \mathrm{i}\boldsymbol{\kappa}q)e^{-\mathrm{i}\boldsymbol{\kappa}\cdot\boldsymbol{x}}$)

$$\tilde{p}(\cdot,t) \in P_\#(\boldsymbol{\kappa},\mathcal{Z}_f) := \{q \in H^1_\#(\mathcal{Z}_f) |\ (\nabla q - \mathrm{i}\boldsymbol{\kappa}q)\cdot\boldsymbol{\nu}^f = 0 \text{ on } \partial_s\mathcal{Z}_f\}\ . \tag{5}$$

The weak formulation of (3) can be established in the standard way using the variational equality,

$$\gamma\rho_0\int_{\mathcal{Z}_f}\frac{\partial^2}{\partial t^2}\tilde{p}\tilde{q} + \int_{\mathcal{Z}_f}\nabla\tilde{p}\cdot\nabla\tilde{q} = \int_{\partial\mathcal{Z}_f}\nabla\tilde{p}\cdot\boldsymbol{\nu}^f\tilde{q}\ , \tag{6}$$

which is to be satisfied by the solution $\tilde{p}(\cdot,t) \in P_\#(\boldsymbol{\kappa},\mathcal{Z}_f)$ and for all $\tilde{q} \in P_\#(-\boldsymbol{\kappa},\mathcal{Z}_f)$, thus the test functions $\tilde{q} = qe^{\mathrm{i}\boldsymbol{\kappa}\cdot\boldsymbol{x}}e^{\mathrm{i}\omega t}$ associated with (4) describe waves propagating in the opposite directions. This choice yields vanishing the right-hand side integral. Due to the zero Neumann condition, the integral on $\partial\mathcal{Z}_f$ reduces immediately to the integral on the periodic part only, $\partial_\#\mathcal{Z}_f$, which vanishes as well due to the periodicity of $\tilde{p}$. Finally, (6) with the substituted Floquet-Bloch wave form (4) presents the eigenvalue problem: Given $\varkappa$, compute ω and $p \in H^1_\#(\mathcal{Z}_f)$ satisfying

$$(\varkappa^2 - \gamma\rho_0\omega^2)\int_{\mathcal{Z}_f}pq + \int_{\mathcal{Z}_f}\nabla p\cdot\nabla q + \mathrm{i}\varkappa\int_{\mathcal{Z}_f}(\nabla p\cdot\boldsymbol{n}q - \boldsymbol{n}p\cdot\nabla q) = 0\ , \quad \forall q \in H^1_\#(\mathcal{Z}_f)\ . \tag{7}$$

2.1. Numerical computing of the wave dispersion

Using a notation self-explaining in the context of the FE method, the following discretized forms are introduced,

$$\int_{\mathcal{Z}_f}\nabla p\cdot\nabla q \overset{\text{FEM}}{\approx} \mathbf{q}^T\mathbf{C}\mathbf{p}\ , \quad \int_{\mathcal{Z}_f}\nabla p\cdot\boldsymbol{n}q \overset{\text{FEM}}{\approx} \mathbf{q}^T\mathbf{Y}\mathbf{p}\ , \quad \int_{\mathcal{Z}_f}pq \overset{\text{FEM}}{\approx} \mathbf{q}^T\mathbf{M}\mathbf{p}\ , \tag{8}$$

where $\mathbf{q}$ and $\mathbf{p}$ represent the nodal DOFs of fields p and q, respectively. Using this approximation in (7), the discretized dispersion equation is obtained,

$$\left[\mathbf{C} + (\varkappa^2 - \omega_k^2\gamma\rho_0)\mathbf{M} + \mathrm{i}\varkappa(\mathbf{Y}^T - \mathbf{Y})\right]\mathbf{p}_k = \mathbf{0}\ , \tag{9}$$

which for a given real wave number $\varkappa$ and the wave direction $\boldsymbol{n}$ yields a real eigenvalue ω_k and the wave mode $\mathbf{p}_k$ representing amplitudes $p(x)$; note that matrix $\varkappa\mathbf{M} + \mathrm{i}\varkappa(\mathbf{Y}^T - \mathbf{Y}) + \mathbf{C})$ is Hermitean, whereby $\gamma\rho_0\mathbf{M}$ symmetric positive definite.

2.2. Homogenization and asymptotics for low frequencies

The periodic homogenization of model (3) considered in the frequency domain provides a modified Helmholtz equation governing the acoustic wave propagation, see e.g. Cioranescu et al. (2018),

$$\nabla \cdot \boldsymbol{A} \nabla p^0 + \frac{\omega^2}{c_f^2} \phi_f p^0 = 0 \,, \tag{10}$$

where ϕ_f is the fluid volume fraction, c_f is the sound speed in the free fluid. The tensor $\boldsymbol{A} = (A_{ij})$ is computed in terms of the corrector functions π^k defined in the representative pore $Y_f = \varepsilon^{-1}\mathcal{Z}_f$ defined by a "zooming" factor $1/\varepsilon$, where $\varepsilon \approx \max_i\{a_i\}$ corresponds to the characteristic dimension of the channels. Note that $Y = \varepsilon^{-1}\mathcal{Z}$ is established accordingly, thus $Y_f \subset Y$. Using the Y-periodic solutions $\pi^k \in H^1_\#(Y_f)$ of the following variational equation,

$$\int_{Y_f} \nabla_y(\pi^k + y_k) \cdot \nabla_y q = 0 \quad \forall q \in H^1_\#(Y_f) \,, \tag{11}$$

the tensor components A_{ij} are computed using

$$A_{kl} = |Y|^{-1} \int_{Y_f} \nabla_y(\pi^k + y_k) \cdot \nabla_y(\pi^l + y_l) \,, \tag{12}$$

where ∇_y is the gradient with respect to to micro-coordinates $y \in Y$.

The wave dispersion analysis is obtained using $p^0 = \hat{p}\exp\{-\mathrm{i}\boldsymbol{\kappa}\cdot\boldsymbol{x}\}$, with $\boldsymbol{\kappa} = \varkappa\boldsymbol{n}$ substituted in (10). Using the free fluid wave number $\kappa_f = \omega/c_f$, the wave number $\varkappa$ of the acoustic waves in the homogenized scaffolds is given by projection of tensor $\boldsymbol{A}$ into the dyadic tensor defined by the wave direction,

$$\varkappa = \kappa_f \sqrt{\frac{\phi_f}{\boldsymbol{A} : \boldsymbol{n} \otimes \boldsymbol{n}}} \,. \tag{13}$$

3. Numerical illustration and discussion

We report numerical results computed for porous structure generated as periodic structures considered also the work by Kruisová et al. (2018). The eigenvalue problem (7) was discretized by the finite element method, as implemented in the software SfePy (Cimrman et al., 2018), leading to the matrix problem (9). The eigenvalues were computed using the ARPACK solver (implicitly restarted Lanczos method, Lehoucq et al. (1998)) through the SciPy package (function `eigsh()`, see Jones et al. (2001)). The shift-invert mode was used to accelerate the calculation of the smallest eigenvalues.

The dispersion analysis was applied to a series of reference periodic cells with diameters of the solid fibres in interval $[0.01, 0.23]$ mm, see Fig. 1, (a). The inviscid fluid parameters were $\gamma = 5 \cdot 10^{-10}$ Pa^{-1}, $\rho_0 = 1000$ kg/m^3. The incoming wave vector direction was $\boldsymbol{n} = [1, 0, 0]^T$, and the wave number range was $\kappa \in [10, 8410]$ m^{-1}, covering the first Brillouin zone with size ≈ 8371 m^{-1}.

In Fig. 1, (b)-(d), we show the dependence of the eigenfrequencies ω (in MHz) on the wave number κ (in mm^{-1}) for three selected diameters of the solid fibres. It can be observed that with decreasing porosity (increasing the fibres diameter) the two lowest modes do not intersect each other and a band gap opens. The solution provided by the homogenized model provides a good approximation only for very small diameters (large volume fractions), or for waves with large wavelengths. Further research is focused on viscous fluids and acoustics in steady flows.

Acknowledgments

This research was supported by project GACR 17-01618S of the Scientific Foundation of the Czech Republic and due to the European Regional Development Fund-Project "Application of Modern Technologies in Medicine and Industry" (No. CZ.02.1.01/0.0/ 0.0/17 048/0007280), and in part by project LO 1506 of the Czech Ministry of Education, Youth and Sports.

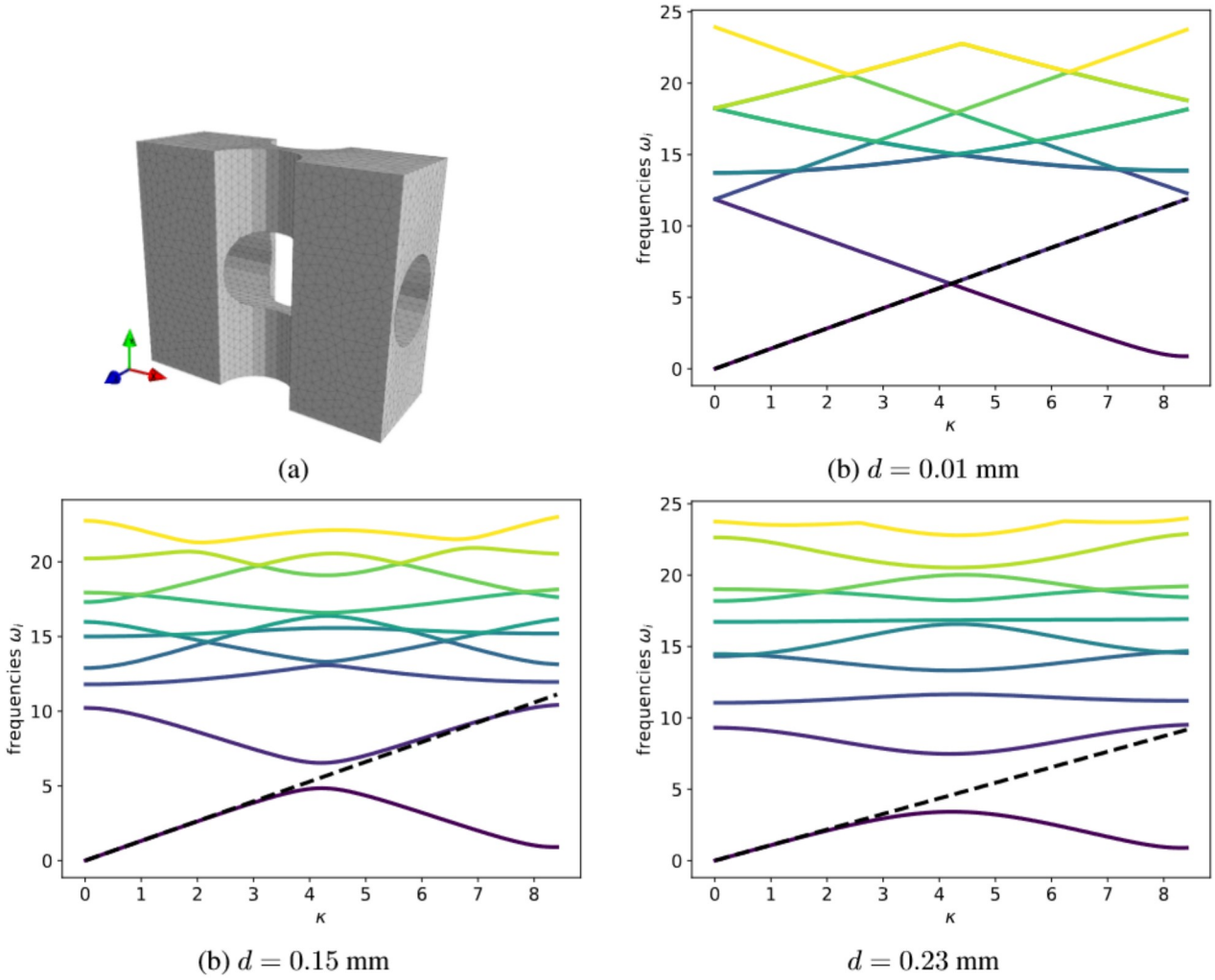

Fig. 1: a) The periodic cell of the microstructure; the gray zone represents the fluid part $\mathcal{Z}_f$. b)-d) The dispersion curves for the microstructure with variable diameter d of the solid fibres. The solid color lines show the dependence of several lowest eigenfrequencies ω (in MHz) on the wave number κ (in mm^{-1}). For a given κ, different curves represent $\omega_k(\kappa)$ computed by solving (9). The dashed lines computed using (13) depict the response $\omega - \kappa$ of the homogenized model.

References

Cimrman, R., Lukeš, V. and Rohan, E. (2018) Multiscale finite element calculations in Python using SfePy, *Advances in Computational Mathematics*, accepted.

Cioranescu, D., Damlamian, A. and Griso, G. (2018) The Periodic Unfolding Method: Theory and Applications to Partial Differential Problems. *Series in Contemporary Mathematics*, Springer Singapore.

Lehoucq, R. B., Sorensen, D. C. and Yang, C. (1998) ARPACK USERS GUIDE: Solution of Large Scale Eigenvalue Problems by Implicitly Restarted Arnoldi Methods. SIAM, Philadelphia, PA.

Jones, E., Oliphant, E., Peterson P. et al.(2001) SciPy: Open Source Scientific Tools for Python, http://www.scipy.org/

Collet, M., Ouisse, M., Ruzzene, M. and Ichchou, M.N. (2011) Floquet-Bloch decomposition for the computation of dispersion of two-dimensional periodic, damped mechanical systems. *International Journal of Solids and Structures*, 48(20):2837–2848.

Sanchez-Palencia, E. (1980) Non-homogeneous media and vibration theory, *Lecture Notes in Physics*, 127, Springer, Berlin.

Kruisová, A. Ševčík, M., Seiner, H. et al.(2018) Ultrasonic bandgaps in 3D-printed periodic ceramic microlattices, *Ultrasonics* 82, 91-100.